proton, thus favoring reduction of the iron and causing the peroxide to be more reducing. This model will explain the rapid redox reactivity of deoxyHr with dioxygen relative to one-electron oxidants.[66] The latter produce rapid one-electron oxidation, but the second oxidation is slow, due either to the rearrangement necessary to make the oxo-bridged ferric site[67] or the poor electron transfer pathway through the hydroxo bridge. The oxidation upon oxygen binding is more rapid, since the bridge proton is removed to form the hydroperoxide, leaving the oxo-bridge. This structure should then be a better electron transfer pathway and be closer to the geometry of the met site, requiring a smaller structural rearrangement.

Acknowledgment. We thank NSF Grant DM8716199 for support of this research. R.L.M. acknowledges support from NIH AREA Grant 1R15GM36481 and thanks Jonathan Efron for his work in sample preparation. P.J.S. thanks the NIH for support of the NIR CD instrument at USC.

Registry No. Fe, 7439-89-6; O_2, 7782-44-7; $[(FeHEDTA)_2O]$, 47821-83-0.

Supplementary Material Available: Text and tables of dimer band energy additivities and optical electronegativities and various met and halfmetHr spectra (9 pages). Ordering information is given on any current masthead page.

(66) Bradic, Z.; Harrington, P. C.; Wilkins, R. G.; Yoneda, G. *Biochemistry* **1980**, *19*, 4149.
(67) (a) Armstrong, G. D.; Ramasan, T.; Sykes, A. G. *Inorg. Chem.* **1985**, *24*, 3230. (b) Armstrong, G. D.; Sykes, A. G. *Inorg. Chem.* **1987**, *26*, 3392. (c) Pearce, L. L.; Kurtz, D. M., Jr.; Xia, Y.; Debrunner, P. G. *J. Am. Chem. Soc.* **1987**, *109*, 7286.

Preresonance Raman Studies of Metal-to-Ligand Charge Transfer in $(NH_3)_4Ru(2,2'\text{-bpy})^{2+}$. In Situ Bond Length Changes, Force Constants, and Reorganization Energies

Stephen K. Doorn and Joseph T. Hupp*

Contribution from the Department of Chemistry, Northwestern University, Evanston, Illinois 60208. *Received June 30, 1988*

Abstract: As a prototype for charge-transfer reactions in general, the intense metal-to-ligand charge-transfer transition occurring in $Ru(NH_3)_4(bpy)^{2+}$ (bpy = 2,2'-bipyridine) has been examined experimentally by resonance and preresonance Raman spectroscopy and analytically by time-dependent scattering theory. To our knowledge, the present example represents the first application of the theory to charge-transfer problems. From the experiments and corresponding theory, the normal-coordinate changes accompanying the transition have been calculated. Both metal–ligand and intraligand bonds are found to distort significantly. When the distortion data are combined with the observed vibrational frequencies, a mode-by-mode assessment of the inner-shell reorganization energy is possible. Further experiments, in which the nature of the solvent is systematically varied, show that selected force constants (and therefore selected components of the internal reorganization energy) are modulated significantly (ca. 6–11%) by ligand–solvent hydrogen bonding. Finally, variations in the nature of the solvent are found to shift ground- and/or excited-state energies in such a way as to either enhance or attenuate the occurrence of net photochemistry.

Outer-sphere electron-transfer reactions, bridge-mediated inner-sphere reactions, and metal–ligand (ligand–metal) charge-transfer reactions constitute a near continuum of interrelated redox processes. Jortner has noted that the dark kinetics and relaxation dynamics of all three can be described in condensed phases by radiationless decay theory.[1] He[1] and others[2] further note that the familiar energy-gap law[3] and Marcus–Hush analysis[4,5] can be viewed as distinct limiting forms of the theory.[6] Regardless of the limiting form, however, nonradiative decay theory asserts that molecular structural changes will exert a profound influence upon the kinetics and dynamics of nearly all charge-transfer processes.

To elaborate, charge-transfer relaxation reactions can be broadly classified as either "weakly coupled" (i.e. highly exothermic, with inverted or nested potential energy surfaces) or "very strongly coupled" (i.e. thermoneutral or only moderately exothermic, with classically intersecting potential energy surfaces).[1,2] Further classification as either inter- or intramolecular (see above) is also possible. For all of these processes the structural changes of interest are the normal-coordinate distortions (Δ) or bond length changes (Δa), which accompany oxidation and reduction or charge redistribution. Collectively the effects of such changes have been handled theoretically in terms of inner-shell or bond reorganization energies (χ_i), where the calculation of χ_i also requires a knowledge of vibrational force constants (f).[4,5]

It should be further noted that any complete analysis of charge-transfer kinetics demands a knowledge of not only the total magnitude of χ_i but also the individual components. The reason for this is that weakly coupled processes make significant use of only high-frequency distortions (as vibrational acceptors for excited-state electronic energy) while strongly coupled processes directly entail only low-frequency distortions (as components of a classical activation barrier).

Obviously, in order to implement radiationless decay theory (or Marcus theory or related theories) as a tool for interpreting charge-transfer kinetics, it is necessary to have a detailed experimental knowledge of χ_i and its components. For very strongly coupled systems[7] the method of choice has been X-ray crystallography[8] (Δa) together with Raman scattering (f). On the other

(1) Jortner, J. *Philos. Mag.* **1979**, *40*, 317.
(2) See, for example: (2) Meyer, T. J. *Pure Appl. Chem.* **1986**, *58*, 1193. (b) Brunschwig, B. S.; Sutin, N. *Comments Inorg. Chem.* **1987**, *6*, 209.
(3) Representative papers: (a) Robinson, G. W.; Frosch, R. P. *J. Chem. Phys.* **1963**, *38*, 1187. (b) Siebrand, W.; Williams, D. F. *J. Chem. Phys.* **1967**, *46*, 403.
(4) Marcus, R. A. *J. Chem. Phys.* **1965**, *43*, 1261.
(5) Hush, N. S. *Prog. Inorg. Chem.* **1967**, *8*, 391.
(6) Energy-gap behavior can be simulated theoretically, for example, by setting all excited-state/ground-state vibrational overlaps (Franck–Condon factors) but one equal to zero. The nonzero overlap is the one involving the $v = 0$ level of the electronic excited state. On the other hand, approximate Marcus-type behavior can be obtained by allowing a nonzero overlap only at the vibrational energy level coinciding with the classical intersection point of the initial-state/final-state potential energy surfaces.
(7) Recent reviews: (a) Sutin, N. *Prog. Inorg. Chem.* **1983**, *30*, 441. (b) Sutin, N. *Acc. Chem. Res.* **1982**, *15*, 275. (c) Marcus, R. A.; Sutin, N. *Biochim. Biophys. Acta* **1985**, *811*, 265. (d) Cannon, R. D. *Electron Transfer Reactions*; Butterworths: London, 1980.

0002-7863/89/1511-4704$01.50/0

hand, for weakly coupled systems the best methods seem to be those based on either low-temperature luminescence (Franck–Condon analysis)[9,10] or excited-state Raman scattering (Badger's rule or other empirical methods).[10,11] While all of these methods appear to give reliable results, their applicability is somewhat limited. Typically, they require special matrices (e.g., single crystals, low-temperature glasses, etc.), special excited-state properties (luminescence, moderate to long lifetimes, photostability, etc.), or other conditions or properties that are unlikely to be available for the majority of interesting systems.

There is a further point: Even when the required conditions can be attained, the resulting structural information may not be fully relevant if the matrix or conditions differ appreciably from those employed in the corresponding kinetics measurements.[12-16] This point has been made most clearly by Curtis and co-workers[14] who have recently shown that χ_i, for at least two systems, can be substantially, and systematically, altered by external ligand–solvent interactions.

Given this situation, there clearly exists a need for additional quantitative approaches to the charge-transfer or redox structure problem. Ideally, any new approach will operate in situ (to take account of environmental effects) and will be capable of high precision, reasonable accuracy, and good sensitivity. One candidate is EXAFS, which indeed is viable as an in situ structural technique. Nevertheless, EXAFS suffers from relatively poor precision (uncertainties of ca. 0.01 Å are typically claimed for Δa in solution[8]) and a notable lack of sensitivity for selected elements and for most bonds remote from the scattering center. Furthermore, because of the need for synchrotron radiation, the technique is, at present, a relatively inaccessible one. Finally, EXAFS has not yet successfully been applied to molecular excited states.

A conceptually different approach is to utilize ground-state vibrational spectroscopic methods. It has long been known, for example, that bond length changes for a given electronic transition can, in principle, be extracted from a resonance Raman excitation profile (Franck–Condon analysis) together with a complete normal-coordinate analysis.[17] (Usually the experiment has been done in the reverse way: structural data have been used to predict Raman spectra.[17]) Unfortunately, excitation profiles, if obtained with suitable resolution, can require a daunting array of spectroscopic instrumentation and a tremendous time investment. Furthermore, the required normal-coordinate analysis may be difficult or nearly impossible for all but the simplest of high-symmetry systems.

Recent theoretical efforts suggest that there may, in fact, exist much simpler spectroscopic methods.[18,19] Specifically, from the work of Heller et al. on time-dependent Raman scattering, there emerge very simple analytical expressions for determining bond length changes or normal-coordinate distortions.[18] For example, under conditions of preresonance excitation, there exists a one-to-one correspondence between Raman scattering intensities (obtained at a single excitation wavelength) and the squares of the bond length changes;[20] with appropriate scaling, Δa values can be extracted. Theoretically the relationships come from a semiclassical picture of wave-packet evolution on an excited-state potential energy surface. Assuming that short-time dynamics accounts for all of the scattered intensity (a condition fulfilled experimentally at preresonance), the time-dependent overlap of the electronic excited-state wave packet with the final, vibrationally excited state of the ground electronic surface is calculated. It is this overlap that gives rise to the scattering. Thus, the term short-time dynamics refers to scattering arising from an initial overlap that decays rapidly and does not recur. From this short-time analysis of the overlaps, the scattered intensity can be related in a simple way to the difference between the ground- and excited-state equilibrium structures.

Heller theory has already been applied with good success to a variety of problems including organic[21] and organometallic photodecomposition and photosubstitution reactions,[22] as well as excited-state bonding studies.[23] The results thus far have been impressive. For example, in a study of d–d chemistry in tungsten–carbonyl complexes, Zink and co-workers were able to detail the contributions of each of 18 vibrational modes, as well as their combinations, to the initial electronic transition.[22d] In view of these remarkable reports, Heller theory would appear to be ideally suited to charge-transfer reactions. There is, for example, a clear promise of unprecedented detail regarding the bond reorganization process, and at an experimental level, the approach should be applicable in almost any environment.

In this article we describe what is apparently the first application of time-dependent Raman scattering theory to charge-transfer reactions. As a prototype transition we chose the intense metal-to-ligand charge transfer occurring in $Ru(NH_3)_4(bpy)^{2+}$. Note that nonradiative decay from $Ru(NH_3)_4(bpy)^{2+*}$ is an example of a *weakly coupled* transition. In a related report we examine a *very strongly coupled* case: intervalence (metal-to-metal) charge transfer in $(NC)_5RuCNRu(NH_3)_5^-$.[24] Despite the distinctions in vibronic coupling, it should be appreciated that the metal-to-ligand and metal-to-metal charge transfers are both basically photodriven intramolecular electron-transfer reactions. Thus, they should provide an experimental base for a more general investigation of redox reactions. Returning to the $Ru(NH_3)_4(bpy)^{2+}$ case, we were motivated in our choice by the availability of independent redox structural data (ground- and excited-state resonance Raman data for the Ru(bpy) fragment;[11] X-ray crystal structures for the ruthenium–tetraamine fragment[25]). We were further motivated by the prospect of tuning ligand(ammine)–solvent interactions in a systematic fashion.[13] Finally, we were hopeful that $Ru(NH_3)_4bpy^{2+}$ would be a photochemically inert system.

The key results of the study are the following: From preresonance Raman experiments, a total of 14 metal–ligand and intraligand modes are found to participate in the reorganization process. When the time-dependent formalism is used, the

(8) An excellent summary of much of the available data for transition-metal complexes is given in: Brunschwig, B. S.; Creutz, C.; Macartney, D. H.; Sham, T.-K.; Sutin, N. *Faraday Discuss. Chem. Soc.* **1982**, *No. 74*, 113.

(9) See, for example: Yersin, H.; Otto, H.; Zink, J. I.; Gliemann, G. *J. Am. Chem. Soc.* **1980**, *102*, 951 and references therein.

(10) Caspar, J. V.; Westmoreland, T. D.; Allen, G. H.; Bradley, P. G.; Meyer, T. J.; Woodruff, W. H. *J. Am. Chem. Soc.* **1984**, *106*, 3492.

(11) Bradley, P. G.; Kress, N.; Hornberger, B. A.; Dallinger, R. F.; Woodruff, W. H. *J. Am. Chem. Soc.* **1981**, *103*, 7441.

(12) Hupp, J. T.; Weaver, M. J. *J. Phys. Chem.* **1985**, *89*, 1601; **1984**, *88*, 1860.

(13) Curtis, J. C.; Sullivan, B. P.; Meyer, T. J. *Inorg. Chem.* **1983**, *22*, 224.

(14) (a) Chang, P. J.; Fung, E. Y.; de la Rosa, R.; Curtis, J. C. *Inorg. Chem.* **1986**, *25*, 4233. (b) Fung, E. Y.; Chua, A.; Curtis, J. C. *Inorg. Chem.* **1988**, *27*, 1294.

(15) Lay, P. A. *J. Phys. Chem.* **1986**, *90*, 878.

(16) Kahn, S. U. M.; Bockris, J. O. In *Chemistry and Physics of Electrocatalysis*; McIntyre, J. D. E., Weaver, M. J., Yeager, E., Eds.; Electrochemical Society: Pennington, NJ, 1984.

(17) Representative work: (a) Van Duyne, R. P.; Suchanski, M. R.; Lakovits, J. M.; Siedle, A. R.; Parks, K. D.; Cotton, T. M. *J. Am. Chem. Soc.* **1979**, *101*, 2832. (b) Jeanmaire, D. L.; Van Duyne, R. P. *J. Am. Chem. Soc.* **1979**, *98*, 4029, 4034.

(18) (a) Heller, E. J.; Sundberg, R. L.; Tannor, D. *J. Phys. Chem.* **1982**, *86*, 1822. (b) Tannor, D.; Heller, E. J. *J. Chem. Phys.* **1982**, *77*, 202. (c) Lee, S. Y.; Heller, E. J. *J. Chem. Phys.* **1977**, *71*, 4777. (d) Heller, E. J. *Acc. Chem. Res.* **1981**, *14*, 368.

(19) See also: (a) Warshel, A.; Dauber, P. *J. Chem. Phys.* **1977**, *66*, 5477. (b) Hizhnyakov, V.; Tehver, I. *J. Raman Spectrosc.* **1988**, *19*, 383. (c) Myers, A. B.; Mathies, R. A. In *Biological Applications of Raman Spectroscopy*; Spiro, T. G., Ed.; Wiley: New York; Vol. 2.

(20) Strictly speaking, this is true only to the extent that a local-mode approximation is valid. More precisely, the theory yields displacements in *normal* coordinates.

(21) Trulson, M. O.; Dollinger, G. D.; Mathies, R. A. *J. Am. Chem. Soc.* **1987**, *109*, 587.

(22) (a) Tutt, L.; Zink, J. I. *J. Am. Chem. Soc.* **1986**, *108*, 5830. (b) Zink, J. I.; Tutt, L.; Yang, Y. Y. *ACS Symp. Ser.* **1986**, *307*, 39. (c) Yang, Y. Y.; Zink, J. I. *J. Am. Chem. Soc.* **1985**, *107*, 4799. (d) Tutt, L.; Tannor, D.; Schindler, J.; Heller, E. J.; Zink, J. I. *J. Phys. Chem.* **1983**, *87*, 3017. (e) Tutt, L.; Tannor, D.; Heller, E. J.; Zink, J. I. *Inorg. Chem.* **1982**, *21*, 3858. (f) Zink, J. I. *Coord. Chem. Rev.* **1985**, *64*, 93.

(23) (a) Yoo, C.-S.; Zink, J. I. *Inorg. Chem.* **1983**, *22*, 2474. (b) Morris, D. E.; Woodruff, W. H. *J. Phys. Chem.* **1985**, *89*, 5795.

(24) Doorn, S. K.; Hupp, J. T. *J. Am. Chem. Soc.* **1989**, *111*, 1142.

(25) Richardson, D. E.; Walker, D. D.; Sutton, J. E.; Hodgson, K. O.; Taube, H. *Inorg. Chem.* **1979**, *18*, 2216.

Table I. Correlated Raman Frequencies for $Ru(NH_3)_4(bpy)^{2+}$ and $Ru(bpy)_3^{2+}$

$Ru(NH_3)_4(bpy)^{2+}$	$Ru(bpy)_3^{2+}$ [11,28a]	assignt
1605	1609	ν(C=C)
1548	1563	
1481	1492	ν(C=N)
	1448	
1331	1320	
1266	1276	
1250	1266	ν(C-C) inter-ring
1172	1176	δ(CCH) in plane
1106	1109	
	1067	
	1040	ring breathing
1027	1030	
767	766	δ(CCH) out of plane
667	663	δ(CCC) inter-ring
456		ν(Ru-NH_3)
376	370	ν(Ru-N(bpy))
248		δ(H_3N-Ru-NH_3)

quantitative role of each can be delineated; the results agree well with those inferred from independent measurements. From studies of scattering as a function of solvent, clear evidence has been obtained for significant external modulation of internal vibrational modes and reorganization energies. Finally, the effects of solvent composition upon net photochemical reactivity are reported.

Experimental Section

Materials. Acetone (AC), acetonitrile (AN), and dimethyl sulfoxide (DMSO) were purchased as analytical-grade solvents from Mallinckrodt. Benzonitrile (BN, 99%), hexamethylphosphoramide (HMPA, 99%), nitromethane (NM, gold label 99+%), and D_2O (99.8%) were obtained from Aldrich. Analytical-grade *N,N*-dimethylacetamide (DMA) was obtained from Baker and nitrobenzene (NB) from Matheson, Coleman, and Bell. All solvents were used without further purification.

$[Ru(NH_3)_5Cl]Cl_2$[26] and $[Ru(NH_3)_5(OH_2)](PF_6)_2$[13] were synthesized according to literature methods. $[Ru(NH_3)_4(bpy)](PF_6)_2$ was prepared via a slight modification of the method of Curtis et al.[13] Typically, 0.31 g (0.64 mmol) of $[Ru(NH_3)_5(OH_2)](PF_6)_2$ was dissolved in 40 mL of argon-degassed acetone. After the solution was stirred for 15 min, 0.10 g (0.65 mmol) of 2,2'-bipyridine was added to the orange solution. The resultant purple solution was stirred under an argon atmosphere for 1 h. The $[Ru(NH_3)_4(bpy)](PF_6)_2$ was collected by filtering the reaction mixture into 6 vol of stirring ether and retrieving the resultant purple-red solid on a frit. The crude product was purified by dissolving in a minimum of reagent-grade acetone, followed by cooling to 0 °C in a freezer. On top of this was layered $^1/_2$ vol of anhydrous ether. The system was allowed to mix overnight by diffusion. The resultant precipitate was recovered on a frit and rinsed several times with ether. (Final yields were typically 25%.) $[Ru(NH_3)_4(bpy)]Cl_2$ was prepared by dissolving 108 mg (0.18 mmol) of the purified $[Ru(NH_3)_4(bpy)](PF_6)_2$ in a minimum of acetone. A solution of 0.38 g (1.4 mmol) of tetrabutylammonium chloride dissolved in a minimum of acetone was added dropwise to the $[Ru(NH_3)_4(bpy)](PF_6)_2$, resulting in the precipitation of its chloride. The dark purple chloride was recovered by filtration and rinsed several times with acetone. (It is slightly soluble in acetone.) No further purification of the $[Ru(NH_3)_4(bpy)]Cl_2$ was carried out.

Raman Measurements. A SPEX 1401 double monochromator system was used to collect the Raman spectra using, typically, a 5-cm^{-1} bandpass. Spectra-Physics Series 2000 Kr^+ and Ar^+ ion lasers were used for sample excitation. Typical laser power was 40–60 mW at the sample. Preresonance Raman spectra were obtained using 647.1- and 676.4-nm excitation from the Kr^+ source on 50 mM solutions of $[Ru(NH_3)_4(bpy)](PF_6)_2$ in HMPA. The spectra taken in the solvent series were obtained at or near resonance using the 514.5-nm line from the Ar^+ source, with 5 mM solutions of the complex. $[Ru(NH_3)_4(bpy)]Cl_2$ was used to prepare the solutions in H_2O and D_2O. All spectra were obtained from a spinning NMR or capillary tube utilizing a 180° backscattering geometry.

Results and Calculations

Raman Spectra. Resonance and preresonance Raman spectra of $Ru(NH_3)_4(bpy)^{2+}$ in HMPA from 200 to 1650 cm^{-1} are shown in Figure 1.[27] These were obtained from a single sample at the excitation energies relative to the MLCT peak maximum as shown in Figure 2. In the spectra, bands due to solvent are marked by asterisks. The broad feature present in the low-energy region of the spectrum taken at 514.5 nm is due to scattering from the glass sample tube.

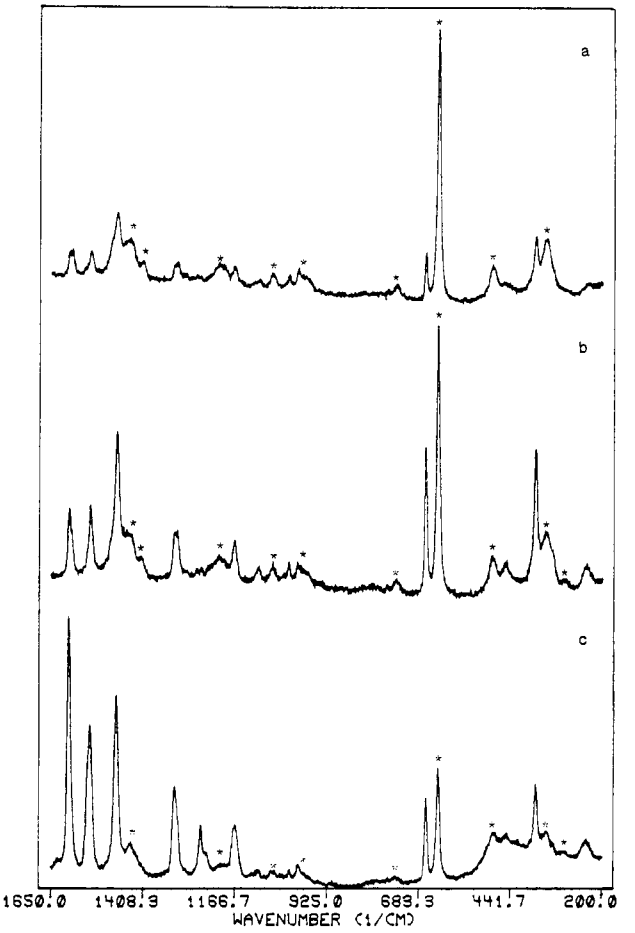

Figure 1. Raman spectra of 50 mM $Ru(NH_3)_4(bpy)^{2+}$ in HMPA as solvent. Excitation wavelengths: (a) 676.6 nm, (b) 647.1 nm, (c) 514.5 nm. Solvent peaks are marked by asterisks.

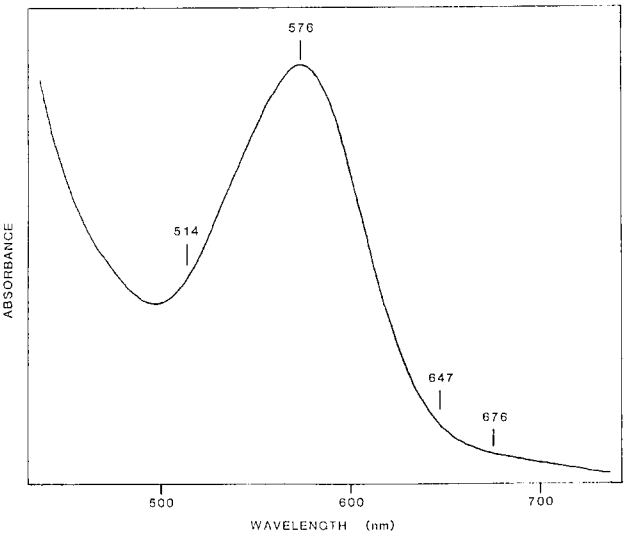

Figure 2. MLCT absorption spectrum of $Ru(NH_3)_4(bpy)^{2+}$ in HMPA.

(26) (a) Vogt, L. H.; Katz, J. S.; Wiberly, S. E. *Inorg. Chem.* **1965**, *4*, 1157. (b) Clarke, R. E. Masters Thesis, The University of California, Santa Barbara, CA, 1978.

(27) The choice of HMPA as solvent is not arbitrary: The MLCT transition in $Ru(NH_3)_4(bpy)^{2+}$ is strongly solvatochromic and HMPA aligns the band in the most optimal way with the available lines for laser excitation (i.e., both resonance and preresonance conditions are easily attained; see Figure 2).

Table II. Effects of Solvent upon E^{MLCT} and Selected Vibrational Modes

solvent	donor no.	E^{MLCT}, cm^{-1}	vibrational energy, cm^{-1} mode 1	mode 2	mode 3
HMPA	38.8	17360	248	456	1548
DMSO	29.8	17830	247	454	1550
DMA	27.8	17920	246	455	1554
H_2O	18.0	19190	237	447	
AC	17.0	18730	241	450	1558
AN	14.1	19120	237	446	1558
BN	11.9	18980	236	444	
NB	4.4	19310	235	442	
D_2O			220	409	
80% NM/ 20% DMSO			247		

Table I lists the frequencies of the observed vibrational modes in $Ru(NH_3)_4(bpy)^{2+}$. A comparison of the bands found for $Ru(NH_3)_4(bpy)^{2+}$ to those observed in the resonance Raman spectrum of $Ru(bpy)_3^{2+}$ shows a close match for many of the modes. A suggested correlation of the observed modes for the two systems, along with assignments of the primary vibrational character of each (discussed below), is also presented in Table I. Band assignments of the intraligand bipyridine modes (appearing above 600 cm^{-1}) have previously been made for $Ru(bpy)_3^{2+}$ based on normal-coordinate calculations performed on bipyridine[28,29] and by comparison with infrared data for similar $M(bpy)_3^{2+}$ systems (where M = Cr, V, and Ti).[30] These bands are attributed to the various totally symmetric C–C and C–N stretches, C–CH in-plane and out-of-plane bends, ring breathing, and inter-ring bending modes. The band appearing at 370 cm^{-1} in the $Ru(bpy)_3^{2+}$ spectrum is generally assigned as the totally symmetric Ru–N(bpy) stretching vibration. It is interesting to note that this band appears quite strongly at 376 cm^{-1} in $Ru(NH_3)_4(bpy)^{2+}$ but is weak for the $M(bpy)_3^{2+}$ (M = Fe, Ru, Os) systems.

The bands found at 456 and 248 cm^{-1} in the spectrum of $Ru(NH_3)_4(bpy)^{2+}$ are not observed for $Ru(bpy)_3^{2+}$. Upon deuteration at the ammonia sites, these shift to 409 and 220 cm^{-1}, respectively. The movement correlates well with the expected magnitude of the difference between $Ru-NH_3$ and $Ru-ND_3$ vibrations. In addition, for a system with C_{2v} symmetry such as $Ru(NH_3)_4(bpy)^{2+}$, group theory permits two totally symmetric $Ru-NH_3$ stretches. Thus, the bands at 456 and 248 cm^{-1} might be assigned to these stretches. Alternatively, the lower energy band could represent (by analogy with infrared assignments)[31] the totally symmetric $NH_3-Ru-NH_3$ bend.

Preresonance Raman scans were also taken in the C–H and N–H stretching region using DMSO-d_6 as the solvent to avoid interference with the broad HMPA bands in this region. No peaks were found between 2750 and 3500 cm^{-1}.

Solvent Effects. Because the MLCT transition in $Ru(NH_3)_4(bpy)^{2+}$ is known to be strongly solvatochromic,[13] we examined the effects of solvent composition on frequencies for Raman scattering. Data were collected near resonance (514-nm excitation) in each of nine solvents (including one mixed system) chosen to encompass the full range of the electronic solvatochromic effect. For most of the vibrational modes the effects of solvent are small (ca. 0–3 cm^{-1}) and comparable in magnitude to the overall measurement precision (ca. 2 cm^{-1}). Thus, their significance is questionable. For three of the modes, however, there are real, measurable solvent-induced effects. Table II lists vibrational frequencies for the two $Ru-NH_3$ vibrations and for the ring-based stretch at ca. 1550 cm^{-1}. For the low- and high-energy metal–ammine modes the maximum solvent-induced frequency shifts are 13 and 14 cm^{-1}, respectively; for the intra-ring mode the largest shift is about half of that. Furthermore, it is worth noting that the frequency shifts are systematic, in the sense that they follow the solvent trend (Table II) for the metal-to-ligand charge-transfer energy (E^{MLCT}).

Besides the nine solvents listed in Table II, we also attempted unsuccessfully to collect Raman data in nitromethane. The reason for failure was traced to a rapid photodecomposition reaction. This complication also exists to a significant extent in acetonitrile, benzonitrile, and nitrobenzene and to a small, but detectable, extent in H_2O as solvent, as shown by a loss of scattered intensity with time. Nevertheless, only in nitromethane was the decomposition severe enough to lead to complete loss of the chromophore following laser illumination. For the remaining four pure solvents, and, interestingly, for a mixture of 80 mol % nitromethane/20 mol % DMSO, there was no detectable chromophore loss under the conditions of our experiment. Moreover, the vibrational frequency of the lower energy $Ru-NH_3$ mode in the mixed solvent system was 247 cm^{-1}—that found for $Ru(NH_3)_4bpy^{2+}$ in pure DMSO.

Calculation of Bond Distortions and Reorganization Energies. The key equation derived by Heller and co-workers[18] to relate Raman scattering intensities to normal-coordinate distortions is the following:

$$\frac{I_1}{I_2} = \left[\frac{V_1}{V_2}\right]^2 \frac{\omega_{2g}}{\omega_{1g}} = \frac{\omega_{1e}{}^3\Delta_1{}^2\omega_{2g}}{\omega_{2e}{}^3\Delta_2{}^2\omega_{1g}} \quad (1)$$

In eq 1, I_1 and I_2 are scattered Raman intensities from vibrational modes 1 and 2, V_k is the vibrational force, ω is 2π times the vibrational frequency, Δ is a unitless distortion of the normal-mode coordinate, and the indices e and g designate, respectively, excited- and ground-state potential energy surfaces. If there are no changes in vibrational frequencies upon electronic excitation or if the changes are sufficiently small to be neglected, eq 1 can be simplified:[18]

$$\frac{I_1}{I_2} = \frac{\Delta_1{}^2\omega_1{}^2}{\Delta_2{}^2\omega_2{}^2} \quad (2)$$

In eq 2, ω now refers to ground-state frequencies. Equations 1 and 2 yield relative normal-coordinate distortions; absolute scalling is available from[13]

$$2\sigma^2 = \sum_k \Delta_k{}^2\nu_k{}^2 \quad (3)$$

where $8\sigma^2$ is the square of the bandwidth at $1/e$ of the peak height for the relevant electronic absorption, ν_k equals $\omega_k/2\pi$, and the summation is over all modes that show intensity in the Raman spectrum.

Thus, from a knowledge of the relative Raman band intensities and their frequencies, coupled with the absorption bandwidth, one can easily calculate the dominant distortions of the normal-mode coordinates accompanying an electronic transition. It is necessary, however, to ensure that (1) short-time dynamics provides the only contribution to the scattered intensity and (2) the observed scattering originates only from resonance (or preresonance) with a single electronic transition. Although for large systems with many active vibrational modes the first condition may be fulfilled with resonance excitation,[18a] we find [based on a comparison of spectra taken with 514- and 647-nm excitation (Figure 1)] that for 514-nm excitation of $Ru(NH_3)_4bpy^{2+}$ the second condition is not fulfilled. The selective enhancement of the seven highest energy bipyridine ring modes found in the 514-nm spectrum suggests that additional enhancement occurs from resonance with the tail of the higher energy $\pi-\pi^*$ electronic transition (see Figure 2).[32] Thus, for $Ru(NH_3)_4bpy^{2+}$ the best prospect for fulfilling

(28) (a) Virdee, H. R.; Hester, R. E. *J. Phys. Chem.* **1984**, *88*, 451. (b) Forster, M.; Hester, R. E. *Chem. Phys. Lett.* **1981**, *81*, 42.
(29) (a) Basu, A.; Gafney, H. D.; Strekas, T. C. *Inorg. Chem.* **1982**, *21*, 2231. (b) Strukl, J. S.; Walter, J. C. *Spectrochim. Acta, Part A* **1971**, *27A*, 209, 223.
(30) König, E.; Lidner, E. *Spectrochim. Acta, Part A* **1972**, *28A*, 1393.
(31) Nakamoto, K. *Infrared and Raman Spectra of Inorganic and Coordination Compounds*, 3rd ed.; Wiley: New York, 1978; p 199.

(32) An alternative or additional explanation would be that enhanced (B-term) scattering occurs via Herzberg–Teller coupling of the MLCT and π^* states.

Table III. Calculated Bond Distortions and Reorganization Energies for the Individual Modes of $Ru(NH_3)_4(bpy)^{2+}$

mode	I_{rel}(cor)	Δ	Δa, Å	χ_i', cm^{-1}
1605	1	0.36	0.0040	100
1548	0.96	0.36	0.0041	100
1481	1.8	0.52	0.0061	200
1331	0.66	0.35	0.0043	82
1266	0.10	0.14	0.0018	13
1250	0.10	0.15	0.0019	14
1172	0.52	0.35	0.0059	73
1106	0.24	0.26	0.0043	36
1027	0.27	0.29	0.0040	43
767	0.12	0.26	0.0054	26
667	2.1	1.2	0.022	520
456	0.27	0.65	0.022	96
376	1.8	2.0	0.048	780
248	0.30	1.3	0.082	200

both conditions is through preresonance excitation. Indeed, a comparison of the spectra taken at 647- and 676-nm excitation shows a uniform increase in intensity of all modes observed in the 647-nm spectrum. Thus, the time-dependent analysis should be applicable to either spectrum.

We have chosen to apply the analysis to the data obtained at 647 nm. The relative vibrational band intensities are listed in Table III. These have been corrected for ν^4 dependence and for absorbance effects according to the method of Shriver and Dunn[33] appropriate for a 180° backscattering geometry. Included in the table are unitless normal-mode distortions obtained from eq 2 and 3, based on $\sigma = 1300 \pm 10$ cm^{-1}.

To convert from a unitless normal-coordinate distortion (Δ) to an apparent bond distortion (Δa) having units of distance, we require either (a) a normal-coordinate analysis, so that the mode distortion can be properly partitioned, or (b) some form of local-mode approximation. We have chosen the latter (however, see Discussion). This leads to

$$\Delta a = (\Delta^2 \hbar / \mu \omega b)^{1/2} \quad (4)$$

where $\hbar$ is Planck's constant divided by 2π, μ is the reduced mass for a particular vibration, and b is the effective bond degeneracy for the vibration. The values we have chosen for b are 4 for the Ru–ammine stretch and 2 for the bend, 2 for Ru–N(bpy), 8 for the C–C–H bends, and 13 for the various ring-based carbon–carbon and carbon–nitrogen bonds taken collectively. (From the available normal-coordinate data,[29] a more detailed local-mode assignment is not justified.) Using these values and appropriate estimates for μ (i.e., 13 for the internal bpy modes, 16 for Ru–NH_3, and 81 for Ru–N(bpy)[34]) in eq 4, the Δa values in Table III are obtained. It should be noted that the apparent bond distortions obtained in this way will not necessarily correspond to actual bond distortions. Even in a local-mode approximation, if b is greater than 1, multiple modes may contribute to a particular bond distortion. If this occurs, the overall distortion (Δr) can be written as

$$(\Delta r)^2 = \sum(\Delta a)^2 \quad (5)$$

where Δa is defined according to eq 4 and the summation is over all modes that involve that particular bond.

From Δa and the appropriate force constant, individual contributions (χ_i') to the inner-shell reorganization energy can be calculated:[7]

$$\chi_i' = \tfrac{1}{2} b (\Delta a)^2 f \quad (6)$$

In eq 6, the force constant is given by

$$f = 4\pi^2 \nu^2 c^2 \mu \quad (7)$$

where c is the velocity of light. Although for complicated systems

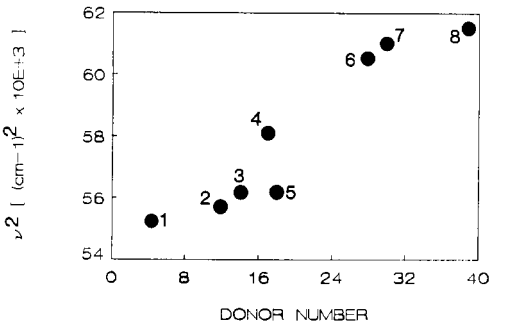

Figure 3. Force constant (as measured by ν^2) for $\delta(H_3NRuNH_3)$ as a function of solvent basicity (donor number) in: (1) NB, (2) BN, (3) AN, (4) AC, (5) H_2O, (6) DMA, (7) DMSO, and (8) HMPA.

b and μ can be difficult to determine, it should be noted that the combination of eq 4, 6, and 7 causes their cancellation:

$$\chi_i' = \tfrac{1}{2} \Delta^2 \nu \quad (8)$$

(In other words, eq 8 permits one to avoid the local-mode approximation.[35]) Table III lists the values of χ_i' obtained from eq 6 or 8.

Discussion

General Observations. Perhaps the most striking aspect of the results in Tables I and III is that 14 separate modes contribute measurably to χ_i. Typically, for inorganic charge-transfer or redox reactions (for example, ground-state metal-centered self-exchanges) χ_i is attributed entirely to one or two ligand–metal stretching modes.[8,36] Table III shows that in the MLCT reaction, ligand–metal modes *are* important in comparison to each of the other modes, but in a global sense they are somewhat less important, comprising less than half of the total reorganization energy. The basis for this result is readily understandable: in the MLCT experiment a nonbonding (metal-localized) $d\pi$ electron is transferred optically to an antibonding π^* orbital, which is delocalized over the entire ring system. As a result a large number of normal-mode coordinates in the ring system are distorted and the balance is such that roughly 53% of the internal reorganization energy is due to distortions in the bipyridine ligand.

A second point is that although 14 modes are active in the preresonance Raman spectrum, an even larger number are allowed but are inactive. Most notably, C–H and N–H stretches are undetectable at preresonance in DMSO-d_6 in the 2750–3500-cm^{-1} region. Although negative results must be interpreted with caution, Heller theory does provide a simple explanation: modes that are not enhanced at preresonance are undistorted by the electronic transition. In terms of reorganization energy, this suggests that the C–H and N–H stretches are not active trapping vibrations for the electronic excited state (cf. Kober et al.[37]).

Solvent Effects. From the existing literature on solvatochromic and electrochemical phenomena in ammine complexes,[12,13,14a,38] the origin of solvent modulation in the metal–ammonia vibrational frequencies is likely to be in ligand–solvent hydrogen-bonding interactions. It has been argued that electron-deficient hydrogens on the ammonias can bind to electron-rich solvent functionalities. Curtis and co-workers have suggested that creation of a hydrogen bond in this way should lead ultimately to an increase in electron density at the metal center, a strengthening of the metal–nitrogen

(33) Shriver, D. F.; Dunn, J. B. R. *Appl. Spectrosc.* **1974**, *28*, 319.

(34) A reduced mass of 81 is appropriate if one takes the vibration at 376 cm^{-1} as the entire bpy ring system vibrating against the rest of the molecule.

(35) The cost, of course, is the loss of information (or assumed information) about the local-bonding nature of the distortion.

(36) On the other hand, Van Duyne and co-workers[12] have shown that, for purely organic systems like tetracyanoquinone(0,−1,−2) and related radical anions, charge transfer involves several modes of reorganization. Our results, together with those from Caspar et al.[10] and from Van Duyne et al., serve to underscore the point that very small distortions for a sufficiently large number of modes can conspire to give a substantial barrier to internal reorganization.

(37) Kober, E. M.; Caspar, J. V.; Lumpkin, R. S.; Meyer, T. J. *J. Phys. Chem.* **1986**, *90*, 3722.

(38) (a) Mayer, V. *J. Electroanal. Chem.* **1979**, *100*, 875. (b) Sahami, S.; Weaver, M. J. *J. Electroanal. Chem.* **1981**, *122*, 171.

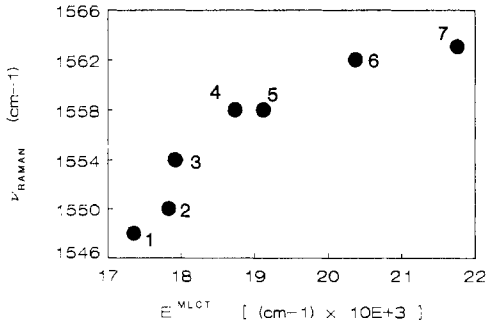

Figure 4. Vibrational frequency of the ν(C=C) mode near 1550 cm^{-1} as a function of MLCT absorption energy maximum for $Ru(NH_3)_4(bpy)^{2+}$ in: (1) HMPA, (2) DMSO, (3) DMA, (4) AC, and (5) AN. Points 6 and 7 are values for $Ru(bpy)_2en^{2+}$ and $Ru(bpy)_3^{2+}$, respectively.[11] E^{MLCT} for $Ru(bpy)_2en^{2+}$ (20 370 cm^{-1}) is for methanol as solvent: Bryant, G. M.; Fergusson, J. E.; Powell, H. K. J. *Aust. J. Chem.* **1971**, *24*, 257.

interaction and a decrease in the metal–nitrogen bond length.[13] Our results provide a direct confirmation of the bond-strengthening effect. Shown in Figure 3 are plots of relative bond strength as measured by the force constant or ν^2 versus the solvent Lewis basicity, as measured empirically by the so-called solvent donor number.[39] The plots show that, indeed, the (internal) metal–ammonia bond strength is greatest when the (external) ligand–solvent hydrogen-bonding interaction is strongest. In principle, preresonance Raman experiments could also provide a test of the bond-compression prediction—or at least a "differential" test in the sense that solvent effects on Δa could be examined. In practice, the precision of our current measurements precludes such an evaluation.

In contrast to the metal–ammine modes, the origin of solvent effects for the bipyridyl mode (1548 cm^{-1} in HMPA) is less obvious. From earlier spectral[40] and electrochemical[41] studies with tris complexes, there is no compelling evidence for specific ligand–solvent interactions. Furthermore, since ammonia lacks π-bonding capabilities, there is no obvious basis for a trans effect, at least as conventionally defined.

An interesting explanation that *does* suffice is one based on energy-gap effects. Caspar et al.[10] have noted from their work on polypyridyl osmium complexes that as the gap between ground- and MLCT excited-state levels decreases, ground-state electronic delocalization between Os^{II} and coordinated (neutral) bipyridine increases, and the bpy ligand begins to acquire significant (ca. 5–15%) radical-anion character. The effect spectroscopically is for the Raman-allowed vibrational modes to shift to slightly lower frequency, consistent with the larger shift (ca. 60 cm^{-1}) that occurs upon complete (one-electron) reduction of uncomplexed bipyridine.[10] In the osmium series the energy gap is manipulated through ligand variations, and although frequency shifts are seen for a number of modes, the largest shifts occur with the mode at 1567 cm^{-1}. (This mode corresponds most closely to the solvent-dependent mode at ca. 1550 cm^{-1} in the tetraammine ruthenium complex.) In the osmium series, an 11-cm^{-1} decrease in vibrational frequency occurs when the energy gap decreases from ca. 20 900 to 14 200 cm^{-1}.

We propose that in our experiments an entirely analogous effect exists, where energy-gap manipulation is achieved through solvent variations. From the E^{MLCT} data given in Table II, the gap between ground and excited states decreases by ca. 1760 cm^{-1} when acetonitrile is replaced by HMPA as solvent. As a direct consequence, delocalization increases and ν (1550 cm^{-1}) decreases. The likely common origin of the ligand- and solvent-based energy-gap effects can be shown nicely by plotting (Figure 4) ν (1550 cm^{-1}) for $Ru(bpy)_3^{2+}$, $Ru(bpy)_2(H_2NCH_2CH_2NH_2)^{2+}$, and, in several solvents, $Ru(bpy)(NH_3)_4^{2+}$ versus the MLCT absorption maximum.

Finally, we note that the energy-gap hypothesis can rationalize one other subtlety in the Raman experiments, namely, the observation that nearly all of the ring-based stretching frequencies in $Ru(NH_3)_4(bpy)^{2+}$ are smaller by a few wavenumbers than those in the corresponding high-energy-gap chromophore, $Ru(bpy)_3^{2+}$.[11] For the latter, metal–ligand orbital mixing should be diminished, and coordinated bipyridine in the ground state should have less $bpy^{\bullet-}$ character.

A second main theme of the solvent studies is reorganization energies. Independent of the detailed explanations (above), the observation of solvent-induced frequency shifts in resonance-enhanced vibrational modes provides unambiguous proof that important internal contributions to the reorganization energy can be modulated by the external environment. To a first approximation, the extent of modulation in χ_i should scale as the vibrational force constant or ν_2. For the low- and high-energy Ru–ammine modes, we find that f can change by as much as 11 and 6%, respectively. For the high-energy bipyridyl mode, f changes by only about 1.3% for the two most extreme solvents. From Table II, the total net effect is that χ_i can be tuned externally only by about 18 cm^{-1}. Such an effect, admittedly, is very small, much smaller, in fact, than that found for a ruthenium tetraammine fragment in recent intervalence experiments.[14a] (χ shifts by ca. 1090 cm^{-1} in the intervalence experiment.)[14a] Clearly, additional effects must exist in the latter experiment. For our experiments, the consequences of solvent tuning in χ_i are so small that they would almost certainly be undetectable in related electron-transfer rate experiments (e.g., $Ru(NH_3)_4(bpy)^{3+/2+}$ self exchange or nonradiative decay from chromophores like $Ru(NH_3)_2(bpy)_2^{2+}$). Nevertheless, the Raman-detected solvent effects are real and their existence implies that significant, detectable rate effects (i.e., factors of 5 or 10) might well exist in systems like $Co(NH_3)_6^{3+/2+}$,[42] where metal–ligand bond distortions are more substantial.

Finally, we want to comment in a qualitative way on the appearance of net photochemistry in the laser photolysis experiments. If the available observations are examined carefully, an interesting demarcation is found with respect to the energetics for creation of the initial excited state. For $E^{MLCT} \leq 18\,730$ cm^{-1}, we observe no net photochemical effects; for $E^{MLCT} \geq 18\,980$ cm^{-1}, we do observe photodecomposition, and at the greatest available energy ($E^{MLCT} = 19\,570$ cm^{-1}; neat nitromethane), photodecomposition is "rapid". Furthermore, we note that if the value of E^{MLCT} in nitromethane is decreased (by the addition of DMSO), photostability is induced.

A survey of the available literature on transition-metal photochemistry reveals that energy-tunable substitution chemistry is a well-established phenomenon. For our purposes, the most relevant work may be that of Malouf and Ford.[43] In a study of pentaammineruthenium(II) complexes they showed that photosubstitution chemistry could be switched on and off by adjusting the MLCT energy through systematic changes in the chromophoric ligands (substituted pyridines and related aromatic heterocycles) and through solvent effects. The explanation was that reactivity is based on access to a nonspectroscopic d–d state. Also, since such states are anticipated to be largely immune energetically to solvent and related effects, access should be controllable based on intersystem crossing, for example, from a tunable MLCT state. Thus, the higher the MLCT state, the more readily accessible will be the photolabile ligand-field state; this is in accord with our observations.

Comparisons to Other Methods. Whenever new structural methods are introduced, it is necessary to evaluate their reliability. One obvious way to do this is by comparison to proven, existing methods. Fortunately, a number of methods have already been applied to ruthenium–ammine and –pyridyl complexes, although not to $Ru(NH_3)_4(bpy)^{2+}$. From these studies data exist that permit

(39) Gutman, V. *Electrochim. Acta* **1976**, *21*, 661.
(40) Kober, E. M.; Sullivan, B. P.; Meyer, T. J. *Inorg. Chem.* **1984**, *23*, 2098.
(41) Sahami, S.; Weaver, M. J. *J. Electroanal. Chem.* **1981**, *122*, 155.
(42) Beattie, J. K.; Moore, C. J. *Inorg. Chem.* **1982**, *21*, 1292.
(43) Malouf, G.; Ford, P. C. *J. Am. Chem. Soc.* **1977**, *99*, 7213.

a critical assessment of the time-dependent Raman method.

In order to identify informative comparisons for similar but nonidentical systems, we note first that, for the metal–ammine fragment in $Ru(NH_3)_4(bpy)^{2+}$, the structural consequences of metal-to-ligand charge transfer should be very similar to those for ground-state one-electron oxidation. Unfortunately, structural data are lacking for the $Ru(NH_3)_4(bpy)^{3+/2+}$ couple; they do exist, however, for a closely related couple, $Ru(NH_3)_4(isn)_2^{3+/2+}$ (isn is isonicotinamide).[25] From X-ray crystallography, Δa for the Ru–N(isn) bond is 0.06 Å. For the Ru–NH_3 bond, Δa is 0.045 Å at the trans position and 0.02 Å at the cis position and the root-mean-square displacement is 0.035 Å. Broadly speaking, our Raman results show fair agreement with these experiments: If we assign the mode at 248 cm^{-1} to bond bending rather than stretching, Δa for Ru–NH_3 (as determined from the 456-cm^{-1} stretching mode) is 0.022 Å and Δa for Ru–N(bpy) is 0.048 Å.

From the comparisons, three points should be noted. First, the observation by Raman spectroscopy that the Ru–polypyridyl nitrogen bond is distorted by more than twice that for Ru–NH_3 is indeed corroborated by the X-ray experiments. These results stand in marked contrast to those for ML_3^{2+} complexes (M = Fe, Os, Ru; L = bpy or 1,10-phenanthroline), where oxidation at the metal center leads to a negligible change in the M–N bond length.[8,44] Second, the Raman-based Δa values are significantly smaller than found for the ground-state isonicotinamide couple. We believe that the differences are real and that a likely explanation is that Δa is diminished in the MLCT experiment because only a fraction of an electron is transferred. Our results (preceding discussion) and those of Caspar et al.[10] are consistent with a fractional charge transfer of, perhaps, 0.6–0.8 electron. The third point is that H_3N–Ru–NH_3 bending (ν = 248 cm^{-1}) evidently plays a more important role in the reorganization of the system than does Ru–NH_3 bond stretching. Furthermore, this role is easily discerned and quantitated in the Raman experiments (Table III). On the other hand, from X-ray experiments the reorganizational cost of bond bending is, in general, not easily assessed. Nevertheless, such measurements do confirm the occurrence of oxidation-state-dependent angular displacements for $Ru(NH_3)_4(isn)_2^{n+}$ in the solid state (typically, 3° for cis ammonia ligands).[25]

Finally, it should be noted that an alternative assignment to bond bending for the mode at 248 cm^{-1} is metal–ammonia stretching. If this is correct, the two-mode Δa value for Ru–NH_3 is 0.062 Å, in substantial disagreement with the ground-state crystallographic measurements. On the basis of the disagreement, we view bond stretching as an improbable assignment.

Evaluation of the bipyridyl data offers an opportunity for distinctly different comparisons. Two techniques have been used previously (and with good success) to obtain excited-state structural information for bipyridyl systems. They are (1) emission spectral fitting (Franck–Condon analysis),[10,37] and (2) Badger's rule applications to ground- vs excited-state vibrational (Raman) frequency shifts.[10] Again, an exact comparison is lacking, but close structural analogies may exist between related chromophoric systems. (A word of caution is appropriate, however. Both techniques give information about "triplet" MLCT states, which may differ structurally from the "singlet" state probed by preresonance Raman.[45])

To illustrate the emission spectral-fitting method, Caspar et al. chose, among other systems, $Ru(bpy)_3^{2+}$, $Ru(bpy)_2(en)^{2+}$, and $Os(bpy)_3^{2+}$.[10] For each of these, low-temperature emission spectra could be fit using a broadened vibrational progression in the range of 1200–1400 cm^{-1} and a second progression at 400 cm^{-1}. These researchers recognized that the apparent progression at ca. 1200–1400 cm^{-1} could contain contributions from any of several modes between 1000 and 1600 cm^{-1}. They also noted, however, that modes in this region would arise chiefly from symmetric C–C and C–N stretching. On this basis, they obtained, by a Franck–Condon analysis, average C–C and C–N bond displacements (MLCT excited state vs ground state) of 0.017, 0.016, and 0.0126 Å for $Ru(bpy)_3^{2+}$, $Ru(bpy)_2(en)^{2+}$, and $Os(bpy)_3^{2+}$, respectively. It is worth noting that the distortions are arranged in decreasing order with decreasing (emissive) energy gap and that this now appears to be a general pattern.[37] For comparison, time-dependent Raman scattering theory yields an apparent average value of $\Delta\bar{a}$ = 0.012 Å for $Ru(NH_3)_4bpy^{2+}$ if all the modes between 1027 and 1605 cm^{-1} are combined (square root of sum of squares). (Inclusion of all modes is implicit in the emission-based Franck–Condon analysis.) In actuality, some of the modes are due predominantly to nonstretching vibrations (see Table I), and if these are omitted, we obtain $\Delta\bar{a}$ = 0.0106 Å. In any case, the agreement between the two types of experiments is remarkable, especially if the likely effects of the diminished energy gap for $Ru(NH_3)_4(bpy)^{2+*}$ are included. (The magnitude of the emissive energy gap for $Ru(NH_3)_4(bpy)^{2+*}$ is unknown, but from the absorption energy gap and comparison to other ruthenium complexes, it probably is slightly smaller than for $Os(bpy)_3^{2+*}$.)

The second excited-state approach[10]—the use of Badger's rule[46]—yields slightly different information. From the difference in ground- and excited-state vibrational frequencies, empirical recipes can be used to extract "apparent" values for the bond-distance displacement using the formula[10]

$$\Delta\bar{r}_{vib} = \ln(\nu/\nu^*)/2.45 \quad (9)$$

where ν and ν^* are, respectively, ground- and excited-state frequencies for a single vibrational mode. In principle, the values for $\Delta\bar{r}_{vib}$ would correspond "exactly" (to the extent that Badger's rule is valid) to individual bond-distance changes, if a local-mode approximation were fully valid. In other words, as applied to the polypyridyl complexes, one assumes that Badger's rule can give a total displacement for each C–C and C–N bond from the measured change in frequency of one normal mode. Actually, because each normal-mode distortion necessarily involves several coupled local coordinate displacements, Badger's rule yields a complicated, weighted-average displacement. Furthermore, this weighted average reflects the relative importance of a particular mode in defining the overall sum of bond distortions. Therefore, different values of $\Delta\bar{r}_{vib}$ (essentially corresponding to the same set of bonds) are to be expected if different normal modes are sampled. Table IV lists values from Caspar et al. for $\Delta\bar{r}_{vib}$ for $Os(bpy)_3^{2+}$. Values for $Ru(bpy)_3^{2+}$ and $Ru(bpy)_2(en)^{2+}$ were obtained from published Raman spectral data[11] using eq 9. Finally, included in the table are $\Delta\bar{r}_{vib}$ values for $Ru(NH_3)_4(bpy)^{2+}$

Table IV. Comparison of Apparent Bond Distance Displacements between Ground and MLCT Excited States for Various Bipyridyl Complexes

	$\Delta\bar{r}_{vib}$ for indicated complex, Å			
mode, cm^{-1}	$Ru(NH_3)_4(bpy)^{2+}$ [a]	$Os(bpy)_3^{2+}$ [b]	$Ru(bpy)_2(en)^{2+}$ [b]	$Ru(bpy)_3^{2+}$ [b]
1605	0.0106	0.0134	0.0134	0.0147
1548	0.0108	0.0122	0.0149	0.0157
1481	0.0161	0.0173	0.0168	0.0174
1331	0.0114	0.0106	0.0103	0.0103
1266	0.0047	0.0158	0.0190	0.0213
1250	0.0050	[c]	[c]	[c]
1027	0.0106	0.0024	0.0088	0.0068
arithmetic average (7 modes)	0.0099	0.0102	0.0119	0.0123
rms average[d] (7 modes)	0.0106	0.0119	0.0128	0.0140

[a] Calculated from time-dependent Raman scattering theory (see text). [b] Calculated from Badger's rule (eq 9) using data from ref 10 and 11. [c] Mode not observed in excited-state Raman spectrum. [d] Note that this average is equivalent to Δr as defined in eq 5.

(44) (a) Zalkin, A.; Templeton, D. H.; Ukei, T. *Inorg. Chem.* **1973**, *12*, 1641. (b) Baker, J.; Englehardt, L. M.; Figgis, B. N.; White, A. H. *J. Chem. Soc., Dalton Trans.* **1975**, 530.

(45) This constraint may be less severe than it appears since spin is a rather poor quantum number for second-row transition metals. Thus, the initially formed "singlet" state should have appreciable "triplet" character and vice versa.

(46) Badger, R. M. *J. Chem. Phys.* **1934**, *2*, 128; **1935**, *3*, 710; *Phys. Rev.* **1935**, *48*, 284.

obtained from our Δa values. The connection between Δa from the Heller analysis and $\Delta\bar{r}_{vib}$ lies in the number of normal modes (m) over which the cost of each local bond distortion is distributed; i.e., $\Delta\bar{r}_{vib} = \Delta a(m)^{1/2}$. For simplicity and for consistency with earlier discussions, m was chosen as 7 for all 13 bonds in the bpy ring system. (Seven symmetric C–C and C–N stretches are expected for coordinated bipyridine.)

From Table IV the following points are evident: (1) The root-mean-square average of $\Delta\bar{r}_{vib}$ for $Ru(NH_3)_4(bpy)^{2+}$ from the Heller analysis (0.0106 Å) matches the value obtained from the same analysis (see above) by combining individual mode distortions, as it must if we have carried out the averaging and summations correctly. (2) There exists a remarkably good correspondence between average apparent bond displacement values from Badger's rule and from the Heller analysis. (3) The "mode-specific" estimates show similarly good agreement, especially for the four highest frequency modes (Table IV). (4) An exception to the general pattern of agreement is the mode at ν = 1266 cm^{-1}. The value from the time-dependent scattering analysis is much smaller than the Badger's rule estimate. The origin of the discrepancy might be in the initial conversion from Δ^2 to Δa in Table III, where we assumed that the normal mode was distributed equally among all 13 C–C and C–N bonds. To the extent that the mode is more correctly perceived as a local mode centered exclusively on the single inter-ring bond, a value of b = 1 (eq 4) will be appropriate. This leads to revised values: Δa (1266) = 0.0065 Å and $\Delta\bar{r}_{vib}$ (1266) = 0.0172 Å. The sensitivity of the Heller method to the choice for b serves to illustrate a significant disadvantage of this analysis in comparison to the excited-state Raman method. Realistic bond length changes will emerge from the former, only when the effective bond degeneracy can be correctly estimated. (On the other hand, if a complete normal-coordinate analysis is available, time-dependent scattering theory should ultimately yield superior estimates for Δr.) (5) The role of the energy gap is evident, once again, in that the average apparent bond displacements, although similar for all systems, are smallest for $Ru(NH_3)_4(bpy)^{2+}$ and largest for $Ru(bpy)_3^{2+}$. (6) It needs to be recognized that each of the various methods ultimately yields slightly different kinds of excited-state information. Perhaps most importantly, the Heller analysis describes vibrational structural differences between the ground state and the initially populated, largely singlet (for ruthenium), excited state. Badger's rule and the emission spectral-fitting method describe differences between the ground state and a collection of lower lying, largely triplet, excited states. The fact that the various results so closely agree suggests that only small differences in vibrational structure or normal coordinates exist for the MLCT singlet versus triplet excited states. (However, see Discussion.)

Given that the Heller analysis does appear to give reliable internal structural information, it is worth considering what advantages it might offer over other methods. (Some disadvantages are discussed in the next section.) First, the new method is potentially far more general than any of the three alternative approaches; it requires neither crystalline substrates nor measurable excited-state properties (however, see next section). Second, the information content is clearly much higher in the preresonance Raman experiment (e.g., 14 active modes for $Ru(NH_3)_4(bpy)^{2+}$) than, for example, in the two-mode emission spectral-fitting experiment. Third, the detailed role of nonstretching modes in the reorganizational process is easily evaluated by the preresonance technique. In contrast, these modes can present difficulties for χ_i determinations based, in particular, on direct X-ray structural measurements.

Further Assumptions. One of the assumptions contained in the simplest recipes from Heller et al.[18] (cf., eq 2) is that ground- and excited-state vibrational frequencies are identical. A corollary is that no mode mixing (Duschinsky rotation) is induced by electronic excitation.[23b] Both assumptions are part of a broader one, which implies that excited-state force constants can be calculated in a simple way from ground-state vibrational data.

For $Ru(NH_3)_4(bpy)^{2+}$ it is unlikely that any of these conditions or assumptions can be completely fulfilled. Time-resolved resonance Raman spectroscopy for $Ru(bpy)_3^{2+}$ and $Ru(bpy)_2(en)^{2+}$ shows, for example, that frequency shifts of 30–60 cm^{-1} can occur between the ground- and excited-state bipyridyl ring modes.[11] In addition, from our current studies of intervalence-enhanced Raman scattering in $(NC)_5Ru^{II}(CN)Ru^{III}(NH_3)_5^-$,[24] frequency shifts of ca. 30 cm^{-1} would be expected for the Ru–NH_3 stretching mode. If mode mixing is absent, these frequency changes can be accommodated by eq 1. For $Ru(NH_3)_4(bpy)^{2+}$ the results are (1) very slight changes in Δ^2 (a few percent or less) and (2) a small degree of reshuffling of the individual components of χ_i. Overall, there is essentially no net effect on χ_i if the frequency-weighted sum of normal-mode distortions continues to be scaled by $2\sigma^2$. We note, however, that the situation is more complex if mode mixing accompanies the frequency shifts. Woodruff and Morris have offered detailed prescriptions for this occurrence, largely in terms of overtone intensity relationships.[23b] Since data of this sort are lacking in our experiments, we forego any further discussion.

A second key assumption is that all modes that contribute significantly to the MLCT bandwidth or to χ are observable in the Raman spectrum. In fact, there almost certainly exists a substantial "Raman-invisible" (due to the proximity of the Rayleigh line) contribution from very low frequency solvent librations.[4] To take this into account, we resort to Hush's theory,[5] which provides an alternative expression for the absorption bandwidth at half-height:

$$\text{fwhm} = 16(\ln 2)kT\chi_{total}^{1/2} \qquad (10)$$

In eq 10, χ_{total} includes both vibrational (χ_i) and solvent (χ_s) effects. For $Ru(NH_3)_4(bpy)^{2+}$, the magnitude of χ_s is difficult to assess in an accurate fashion, but by analogy with $Ru(bpy)_3^{2+}$,[40] 700 cm^{-1} can be taken as a useful guess. If we use this value to diminish χ_{total} in eq 10, the bandwidth in the absence of solvent is estimated to be 300 cm^{-1} less, and σ is ca. 130 cm^{-1} less than in the presence of solvent. From eq 3 and 4, the final effect upon Δa should be a diminution by about 10%. We note that this somewhat cumbersome excursion into the classical theory of Hush is necessary because the relevant spectroscopic expression (eq 3) is designed to accomodate only vibrational effects. In principle, and with a more elaborate theory, nonvibrational solvent contributions could probably be directly included in expressions like eq 2 through damping terms. These would effectively broaden the absorption envelope by adding width to the individual vibrational components.

One further assumption is that the observed absorption band corresponds to a single electronic transition. Actually, because of substantial spin–orbit coupling for Ru(III), the nonbonding $d\pi^5$ manifold in the excited state can be created (by light absorption) in three energetically distinct forms. In fact, for $Ru(bpy)_3^{2+}$, the individual transitions are partially resolved in the electronic absorption spectrum, and from spectral fitting and related techniques, the energy splittings and individual intensities can be determined.[47] For $Ru(NH_3)_4(bpy)^{2+}$, the absorption envelope is a structureless Gaussian, so detailed information is not as easy to obtain. One solution would be to obtain polarized absorption spectra on single-crystal specimens. A simpler, but much more crude, solution is to carry out spectral simulations. If two conditions are imposed on the simulation—namely, equal component bandwidths and an absence of overall structure—we encounter the following: For any reasonable combination of individual band intensities and energy spacings, a spectrum is generated in which each individual component is narrower (at half-height) than the overall envelope by, typically, 100–300 cm^{-1}.

It needs to be appreciated that the above approach is a nonrigorous one; by no means have we obtained a unique range of solutions. Nevertheless, these results may be suitable for illustrative purposes. If 300 cm^{-1} is taken as an appropriate upper limit correction to the absorption bandwidth, then the scaling factor, σ, decreases by ca. 130 cm^{-1}. As a direct consequence, χ_i decreases by 20% and Δa by about 10%. Thus, in combination with the solvent correction, our initial calculations could be in error

(47) Kober, E. M.; Meyer, T. J. *Inorg. Chem.* **1982**, *21*, 3967.

(on the high side) by up to 40% for χ_i and 20% for Δa. To the extent that these errors exist, our conclusion regarding the very close structural similarity between MLCT singlet and triplet excited states will need to be modified.

Concluding Remarks

Despite the caveats, the preresonance technique in combination with the time-dependent analysis appears to provide a powerful and reliable approach to charge-transfer structural measurements. Normal-coordinate distortions derived from preresonance Raman agree reasonably well with those that can be inferred from other methods. For the $Ru(NH_3)_4(bpy)^{2+}$ case, the precision and sensitivity are nothing short of remarkable. Separate studies with $(NC)_5Ru(CN)Ru(NH_3)_5^-$ tend to reinforce these conclusions.[24] Clearly, it will be necessary, however, to examine additional systems before the hoped-for generality of the new approach can be firmly established. Of particular interest in such an effort will be studies of symmetrical mixed-valence systems, outer-sphere (ion-paired) systems, and systems featuring spin-orbit allowed triplet transitions.

Acknowledgment. We thank Professors Jim Kincaid, Mark Ratner, David Tannor, and Rick Van Duyne for useful comments. This work was supported by the United States Department of Energy, Office of Energy Research, Division of Chemical Sciences (Grant No. DE-FG02-87ER13808), and in its initial stages by a Junior Faculty Fellowship from the Atlantic-Richfield Foundation. The Raman facility is part of the Northwestern University Materials Research Center and is supported by a grant from NSF (DMR-8520280).

Alkoxy and Aryloxy Derivatives of (Pentamethylcyclopentadienyl)ruthenium. X-ray Crystal Structures of $[(\eta^5\text{-}C_5Me_5)Ru(\mu\text{-}OMe)]_2$, $[(\eta^5\text{-}C_5Me_5)(CO)Ru(\mu\text{-}OEt)]_2$, and $(\eta^5\text{-}C_5Me_5)Ru(\eta^5\text{-}2,6\text{-}{}^tBu_2C_6H_3O)$ and Molecular Orbital Analysis of $[(\eta^5\text{-}C_5H_5)Ru(\mu\text{-}OMe)]_2$

Stefan D. Loren,[†] Brian K. Campion,[†] Richard H. Heyn,[†] T. Don Tilley,*[,†] Bruce E. Bursten,*[,‡] and Karl W. Luth[‡]

Contribution from the Chemistry Department, D-006, University of California at San Diego, La Jolla, California 92093-0506, and the Department of Chemistry, The Ohio State University, Columbus, Ohio 43210-1173. *Received August 15, 1988*

Abstract: Ruthenium methoxide dimer $[Cp^*Ru(\mu\text{-}OMe)]_2$ (**1**, $Cp^* = \eta^5\text{-}C_5Me_5$) is produced by reaction of $[Cp^*RuCl_2]_2$ or $Cp^*RuCl_2(pyr)$ with NaOMe in methanol or by reaction of $Cp^*(PCy_3)RuCl$ with LiOMe in methanol. Compound **1** is best prepared in pure form (in 84% yield) by reaction of the tetranuclear cluster $[Cp^*RuCl]_4$ with 4 equiv of LiOMe in methanol. An X-ray crystallography study revealed that **1** has a dimeric structure with bridging methoxy ligands. The dimer is folded along the O···O axis, with a fold angle of 124.3°. Complex **1** crystallizes in the monoclinic space group $C2/c$ with a = 15.821 (8) Å, b = 6.659 (3) Å, c = 21.51 (1) Å, β = 103.32 (3)°, Z = 8, V = 2205 (2) Å^3, and R_F = 2.17%. Ethoxide dimer $[Cp^*Ru(\mu\text{-}OEt)]_2$ (**2**), prepared from $[Cp^*RuCl]_4$ and LiOEt in ethanol, combines with carbon monoxide to form the adduct $[Cp^*(CO)Ru(\mu\text{-}OEt)]_2$ (**3**). Compound **3** crystallizes in tetragonal space group $P\bar{4}2_1c$ with a = 26.22 (2) Å, c = 8.709 (5) Å, Z = 8, V = 5986 (6) Å^3, and R_F = 5.68%. An analogous adduct of **1**, $[Cp^*(CO)Ru(\mu\text{-}OMe)]_2$ (**4**), is observed by ^1H NMR but is unstable in solution, eventually decomposing to $[Cp^*Ru(CO)(\mu\text{-}CO)]_2$. Reaction of LiO-2,6-$^tBu_2C_6H_3$ with $[Cp^*RuCl]_4$ in toluene gives the η^5-oxocyclohexadienyl complex $Cp^*Ru(\eta^5\text{-}2,6\text{-}{}^tBu_2C_6H_3O)$ (**5**), which was crystallograpically characterized. Compound **5** crystallizes in space group $P2_1/n$ with a = 12.203 (3) Å, b = 10.028 (3) Å, c = 18.414 (4) Å, β = 99.11 (2)°, Z = 4, V = 2225 (1) Å^3, and R_F = 3.03%. The electronic structure of an analogue of **1**, $[CpRu(\mu\text{-}OMe)]_2$ (**1'**, $Cp = \eta^5\text{-}C_5H_5$), was investigated by using Fenske-Hall molecular orbital calculations. These studies show that the folded C_{2v} structure of **1** is due to electronic preferences of the bridging alkoxide ligands. Upon folding, lone-pair orbitals of appropriate symmetry on the bridging oxygen atoms maximize their donation into the unoccupied Ru orbitals.

Recent interest in the preparation and study of noble metal (Ru, Os, Rh, Ir, Pd, and Pt) alkoxide and aryl oxide derivatives stems from the paucity of examples and what appears to be an inherently rich reaction chemistry.[1] Currently alkoxide or aryl oxide derivatives of all of these metals have been described, but there are relatively few investigations of the chemistry of these species.[1-12,15-17] In an attempt to obtain a ruthenium alkoxide, Wilkinson and co-workers studied the reaction of $RuHCl(PPh_3)_3$ with sodium methoxide. This investigation showed that methoxide complexes in this system are thermally unstable and that decomposition products include formaldehyde, formyl, and carbonyl derivatives.[2]

A number of bonding modes for alkoxy and aryloxy ligands on ruthenium have now been identified. Yamamoto prepared the terminal alkoxide $RuH[OCH(CF_3)Ph](PPh_3)_3$ by insertion of trifluoromethyl phenyl ketone into the Ru-H bond of RuH_2-

[†] University of California at San Diego.
[‡] The Ohio State University.

(1) Leading references include: (a) Mehrotra, R. C. *Adv. Inorg. Chem. Radiochem.* **1983**, *26*, 269. (b) Newman, L. J.; Bergman, R. G. *J. Am. Chem. Soc.* **1985**, *107*, 5314. (c) Bryndza, H. E.; Calabrese, J. C.; Marsi, M.; Roe, D. C.; Tam, W.; Bercaw, J. E. *Ibid.* **1986**, *108*, 4805. (d) Braga, D.; Sabatino, P.; Di Bugno, C.; Leoni, P.; Pasquali, M. *J. Organomet. Chem.* **1987**, *334*, C46. (e) Michelin, R. A.; Napoli, M.; Ros, R. *Ibid.* **1979**, *175*, 239. (f) Yoshida, T.; Okano, T.; Ueda, Y.; Otsuka, S. *J. Am. Chem. Soc.* **1981**, *103*, 3411. (g) Carmona, D.; Oro, L. A.; Lamata, M. P.; Puebla, M. P.; Ruiz, J.; Maitlis, P. M. *J. Chem. Soc., Dalton Trans.* **1987**, 639. (h) Bernard, K. A.; Atwood, J. D. *Organometallics* **1987**, *6*, 1133. (i) Kullberg, M. L.; Kubiak, C. P. *Ibid.* **1984**, *3*, 632. (j) Paonessa, R. S.; Prignano, A. L.; Trogler, W. C. *Ibid.* **1985**, *4*, 647. (k) Abel, E. W.; Farrow, G.; Towie, I. D. H. *J. Chem. Soc., Dalton Trans.* **1979**, 71. (l) Komiya, S.; Tane-ichi, S.; Yamamoto, A.; Yamamoto, T. *Bull. Chem. Soc. Jpn.* **1980**, *53*, 673. (m) Arnold, D. P.; Bennett, M. A. *J. Organomet. Chem.* **1980**, *199*, 119. (n) Rees, W. M.; Fettinger, J. C.; Churchill, M. R.; Atwood, J. D. *Organometallics* **1985**, *4*, 2179.

0002-7863/89/1511-4712$01.50/0